Stabilization Effects of Real Gas for Cellular Detonations

Zifeng Weng[a], Rémy Mével[b], Zhuyin Ren[c], Shijin Shuai[a,c]
[a] School of Vehicle and Mobility, Tsinghua University, Beijing, 100084, China
[b] School of Aeronautics and Astronautics, Zhejiang University, Hangzhou, 310027, China
[c] Institute for Aero Engine, Tsinghua University, Beijing, 100084, China

1 Motivations

Detonation is an intrinsically unstable combustion wave. In multi-dimension, the detonation dynamics is governed by the longitudinal and transverse instabilities. Transverse shock wave sweeps along the detonation front and results in the formation of cellular structures. Theoretical analysis on detonation stability was pioneered by Erpenbeck [2, 3] based on linear stability analysis (LSA) and Laplace transformation. Their approach enables to determine the stability of a given mixture and interpolate the locations of neutral stability. Erpenbeck's method was improved by Lee et al. [5] who introduce the normal mode approach for the LSA of 1D pulsating detonation. This technique was extended by Short et al. [9] to 2D cellular detonation. Generally, the neutral stability boundary and the variation of eigenfunctions can be theoretically derived following their approaches. These theoretical results were shown to agree well with a number of cellular detonation simulations [1, 7, 8, 12]. One major limitation is the ideal gas or perfect gas (PG) assumptions which are limited to low-pressure conditions. At elevated pressure, the real gas (RG) effects, including the finite molecular volume and intermolecular attraction force, become non-negligible. Recent simulations performed by Taileb et al. [10] show that the finite molecular volume significantly enhances the regularity of cellular structure. Weng et al. [13] conducted LSA for pulsating detonation, accounting for the effect of finite molecular volume, and confirmed the stabilization effect. However, theoretical analysis for the stability of cellular detonation in real gas has not been performed. Gorchkov et al. [4] have proposed the formulations of LSA for arbitrary equations of state (EoS) and multi-step reactions but their approaches have not been applied to RG EoS. In addition, the effect of intermolecular attraction has not been considered in previous works. This study aims at extending Short et al.'s LSA [9] from PG to RG, with both the finite molecular volume and intermolecular attraction force considered. Numerical simulations were also performed to validate and complement the theoretical analysis.

2 Methodologies

The reaction zone structure of the detonation is governed by the reactive Euler equations

$$\frac{Dv}{Dt} - v\nabla^l \cdot \boldsymbol{u}^l = 0, \quad \frac{D\boldsymbol{u}^l}{Dt} + v\nabla^l P = 0, \quad \frac{DP}{Dt} + \frac{c^2}{v}\nabla^l \cdot \boldsymbol{u}^l = \frac{c^2}{v}\dot{\sigma}, \quad \frac{D\lambda}{Dt} = \dot{r}. \tag{1}$$

Correspondence to: mevel@zju.edu.cn

The superscript l denotes a variable in the laboratory coordinate. t is time, v is the specific volume and $\boldsymbol{u}^l$ is the velocity. The energy equation has been replaced with the adiabatic change equation to use pressure (P) instead of internal energy (e) as a primitive variable. c and $\dot{\sigma}$ are the sound speed and thermicity, respectively. For the ease of theoretical study, a one-step irreversible reaction, $\mathcal{R} \rightarrow \mathcal{P}$ was considered. λ is the mass fraction of the product, which also corresponds to the reaction progress variable. $\dot{r}$ is the net production rate,

$$\dot{r} = K\phi Z(1-\lambda)\exp\left(-E/T\right), \tag{2}$$

where K is the pre-exponential factor; ϕ is the fugacity coefficient of the product; Z is the compressibility factor of the mixture; E is the activation energy. The non-ideality of RG at elevated pressure was described with the Redlich-Kwong (RK) and Noble-Abel (NA) EoS. The RK EoS reads

$$P = \frac{T}{v-B} - \frac{A(T)}{v^2+Bv}, \quad A(T) = 0.42748\frac{T_c^{2.5}}{P_c T^{0.5}}, \quad B = 0.08664\frac{T_c}{P_c}. \tag{3}$$

It reduces to the NA EoS when setting A to zero. The effects of inter-molecular attraction and finite molecular volume were accounted for with the attraction (A) and covolume parameters (B), respectively. These two parameters are related to the critical temperature (T_c) and critical pressure (P_c) of a given species. It was assumed that the reactant and product have the same A and B values.

In the LSA, small perturbation was applied to the steady solution, i.e., the ZND model. Based on the normal mode approach, the state vector $\boldsymbol{z} = (v, u, w, P, \lambda)^T$ was defined and linearized as

$$\boldsymbol{z} = \boldsymbol{z}^* + \boldsymbol{z}'(x)\exp(\alpha t + \mathrm{i}ky), \quad \psi = \exp(\alpha t + \mathrm{i}ky), \tag{4}$$

where the superscript * refers to values of the ZND model; α, z' and ψ_0 are all complex; k is the wave number. α is given as $\alpha_r + \alpha_i\mathrm{i}$ with α_r being the growth rate and α_i being the frequency. The governing equation can be linearized as

$$\boldsymbol{A}^*\boldsymbol{z}'_x + (\alpha + \mathrm{i}k\boldsymbol{B}^* + \boldsymbol{C}^*)\boldsymbol{z}' - \alpha\boldsymbol{z}^*_x + \mathrm{i}k\boldsymbol{e}^* = 0, \tag{5}$$

The equation was closed by two boundary conditions; one is the linearized Rankine-Hugoniot relation behind the shock, and the other one is the radiation condition at the end of the reaction zone [4, 5, 9]. This two-boundary problem was then solved with a shooting algorithm proposed by Lee et al. [5].

The numerical simulations were conducted with an in-house solver RSDFoam, developed for RG shock and detonation simulation [11]. Quadratic MUSCL and an approximate HLLC Riemann solver were utilized for the reconstruction and flux calculation at the grid interface. The time integration was conducted with a third-order, strong-stability-preserving Runge-Kutta method. The CFL number was 0.2. The RG model was implemented in Cantera which also handles the chemistry with the CVODE integrator. A square domain of 150×150 was used. The solution of the ZND model was filled in the left 50 grid points of the domain without prescribed perturbation. At the left boundary, outflow conditions were applied, while at the right boundary, an inflow with constant velocity of $0.95D^*$ was imposed. Top and bottom boundaries were adiabatic slip walls. The size of the base mesh was $l_{1/2}$/6 and three levels of mesh refinement were applied based on the density gradient, which results in the finest mesh of $l_{1/2}$/48. The detonation was allowed to run for more than 1000 $l_{1/2}$. The mixture properties are summarized in Table 1.

Table 1: Properties of mixtures for the cellular detonation simulations with PG and RG models.

EoS	$A(T_1)$	B	θ	M	Q	E	Stability
PG	0	0			31.4182	15.1878	Unstable
NA	0	0.2	4.3902	5.0	31.4182	15.1878	Unstable
RK	0.6	0.2			16.7793	10.5429	Stable

3 Results

Figure 1 presents the complete neutral stability boundary for 2D cellular detonation in RG. The 1D and 2D stability boundaries of PG were also plotted as references. In the E-Q plane, the appearance of transverse instability changes the neutral stability boundary from C-shape in 1D to hyperbola-like in 2D, which significantly reduces the parameter space of stable detonation. There is a maximum Q, i.e., 11.52, in the 2D boundary which corresponds to a maximum Mach number (M) in the M-θ plane. This Mach number was named as $M_{\mathrm{2D,max}}(= 3.22)$ in this work. With the RG effects, the neutral stability boundary for 2D cellular detonation reverses back to a C-shape in the E-Q plane, and covers a much wider range of Mach number in the M-θ plane. In the small Q range, the 2D stability boundary of RG is close to the perfect gas one. As Q increases, the stabilizing effect of RG becomes more significant. The finite molecular volume has dominant impact on the variation of the stability boundary. Nonetheless, as the inter-molecular attraction force is included, it shifts the neutral stability boundary to the stable side, and thus further stabilizes the detonation. In the M-θ plane, the critical reduced activation energy of RG does not decreases monotonically with M as the PG one. Instead, it firstly decreases and then increases with the Mach number. Again, a stabilizing effect was observed.

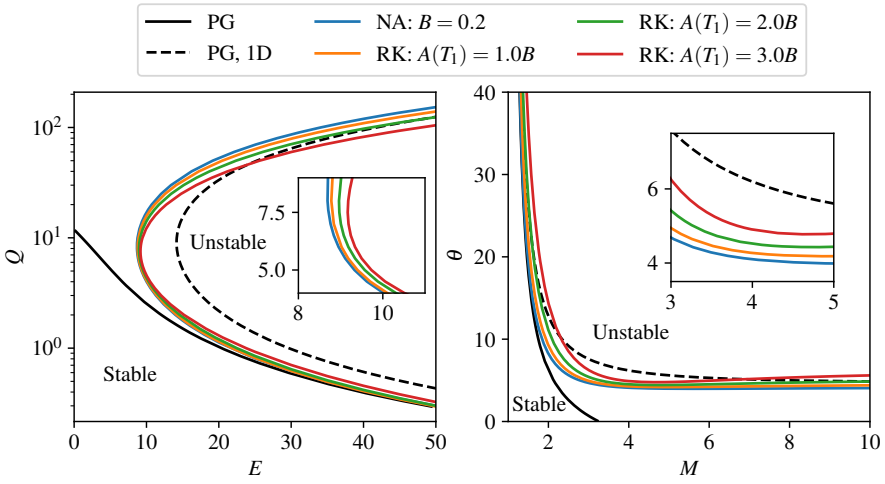

Figure 1: Neutral stability boundary in E-Q and M-θ for 2D detonation obtained with RG models. The 1D and 2D stability boundaries of PG were also plotted as references. B was fixed at 0.2 for RK model.

Weng et al. [12] have defined four regimes of stability using the 1D and 2D stability boundaries in the M-θ plane for PG model. The definitions and characteristics of the four regimes are as follows. (0) Stable region: on the left of the 2D stability boundary; the detonation is steady and planar. (1) Linear instability: between the 1D and 2D stability boundary, with Mach number smaller than $M_{\mathrm{2D,max}}$; the detonation is characterized by regular cellular structure and the size can be well predicted with the most unstable wavelength in LSA. (2) Weakly nonlinear instability: between the 1D and 2D stability boundary, with Mach number larger than $M_{\mathrm{2D,max}}$; the detonation has regular cellular structure but the cell size increases as detonation propagates and the valid of the prediction from LSA is limited to the initial stage of cell formation. (3) Nonlinear instability: beyond the 1D stability boundary; there is rapid transition from steady planar detonation to cellular detonation due to interaction between longitudinal and transverse instabilities, large perturbations introduced by local explosions, appearance and dominance of high-frequency modes of transverse instability. The stability map was extended from PG to RG in Fig. 2. When only the finite molecular volume was considered, the stability boundaries at the large θ limit are close to the PG ones. Due to the disappearance of $M_{\mathrm{2D,max}}$ in the 2D stability boundary, the

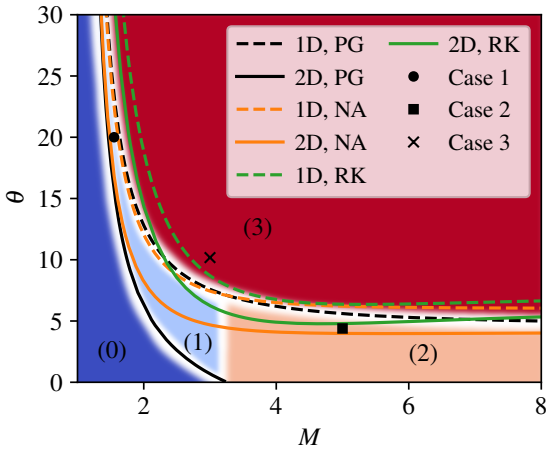

Figure 2: 1D and 2D neutral stability boundaries for PG and RG. The stability map is defined for PG. NA: $B = 0.2$. RK: $A(T_1) = 3B$. Symbols denote the simulation conditions.

stable region (0) extends to much higher Mach number, and regimes (1) and (2) cannot be clearly separated. The 2D boundary of NA penetrates into region 3 of PG in the large M limit, which decreases the area of region (3) for NA. A nonlinearly unstable detonation for PG can thus become weakly nonlinear in the NA case. By additionally including the effect of inter-molecular attraction force, the 1D and 2D boundaries of RK EoS are dramatically shifted toward region (3) of PG. In the large θ limit, the linear instability region (1) of RK falls in the nonlinear instability region (3) of PG. Similarly, in the large M limit, the weakly nonlinear instability region (2) of RK also overlaps with the nonlinear instability region (3) of PG. Again, regions (1) and (2) are difficult to differentiate as in the NA case. The dynamics of detonation of RG in these two regions are further studied via numerical simulations.

The numerical simulations considered three mixtures as denoted in Fig. 2 with cases 1 to 3. In the following, results of case 2 are mainly shown and discussed and the setup is detailed in Table 1. Fig. 3 presents the transient fields for case 2 at $t = 160$. In the PG simulation, there is large difference in the strength of the incident shock and the Mach stem which results in a strong shear flow around the slip line. Due to the onset of Kelvin–Helmholtz instability, vortices are generated at the shear flow as shown in the temperature and schlieren fields. In addition to the main triple point at the detonation front, a second triple point is also observed downstream in the pressure field. These structures are consistent with experimental results for weakly unstable detonation, like hydrogen–oxygen with large argon dilution [6]. As the effect of the finite molecular volume is included, the detonation is significantly stabilized. The detonation front is less perturbed compared to the PG case. Around the slip line, no obvious vortex can be observed. In the temperature or schlieren fields, the vortical flow behind the detonation in the PG case is replaced by a number of cell patterns in the NA case. In the RK case, a completely planar detonation is obtained, which agrees with the prediction of LSA.

Figure 4 shows the numerical soot foil and distribution of cell size in PG and NA cases. In the PG case, the cellular structure can be observed around $x = 100$ (not shown). The cell size is quite small at the birth of the cellular structure. As the detonation propagates, the cell size grows and stabilizes at a larger value. The cell size was measured in the range 950 to 1050. The average cell size is 17.95 ± 3.51, which is 163% larger than the prediction with LSA, i.e., 6.82. The cell shows irregular distribution with the maximum size of 23.58 and the minimum size of 8.48. According to the findings in our previous work [12], the LSA predicts better the cell size formed at early stage around $x = 100$. During the detonation propagation, the nonlinear dynamics of the detonation get progressively excited and leads to larger cellular structures. In the NA case, the appearance of the cellular structure is significantly delayed

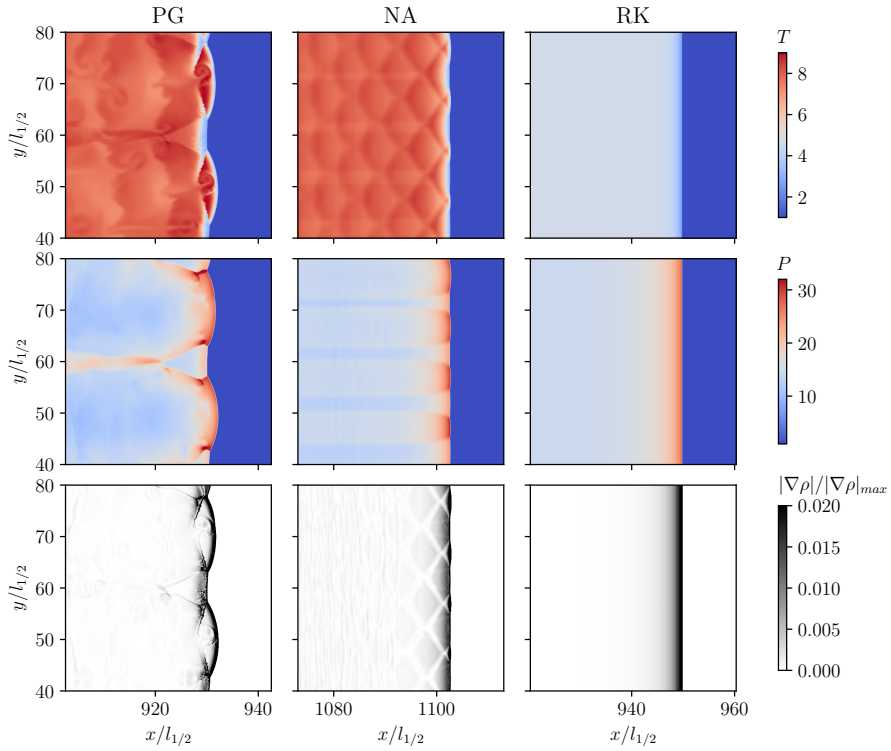

Figure 3: Temperature, pressure and schlieren fields for case 2 at $t = 160$.

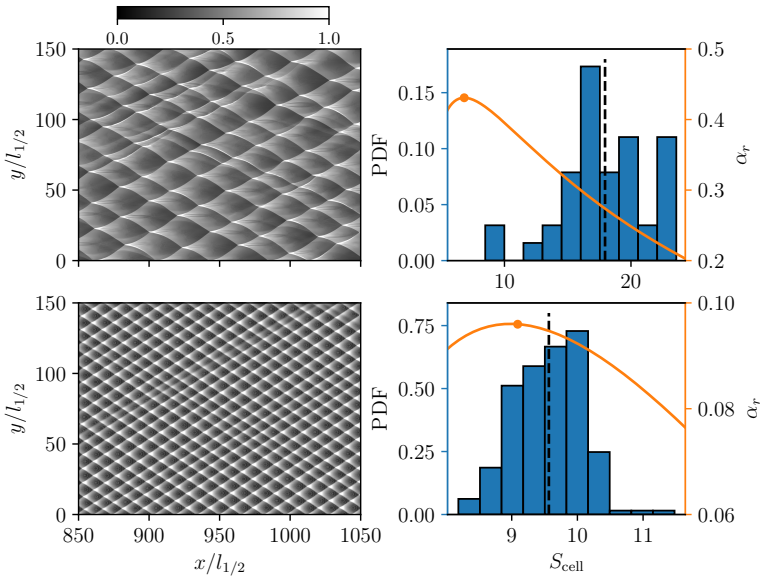

Figure 4: Numerical soot foil and PDF of cell size for case 2. Top: PG model; bottom: NA model. The black dash lines denotes the average values which are 17.95 (PG) and 9.57 (NA). The orange curve and circle denote the growth rate and prediction of cell size obtained in LSA, respectively.

due to the stabilizing effect of real gas. Moreover, no obvious growth of the cell size is observed in the simulation. The cellular structure is very regular with cell size ranging from 8.19 to 11.48. The average cell size is 9.57±0.51, which agrees well with the prediction of LSA, i.e., 9.09. These characteristics

are actually more similar to those of regime (1). Recalling the definition of regimes (1) and (2) in the stability map, they were separated by $M_{\mathrm{2D,max}}$ in the PG case. Since $M_{\mathrm{2D,max}}$ disappears in the LSA of the NA case, it should be expected that regime (2) would be completely replaced by regime (1). The variation of the stability map thus explains the change of cellular dynamics in the NA case as compared to the PG case.

In summary, the stabilization effects of both the finite molecular volume and inter-molecular attraction force were revealed for cellular detonation via theoretical analysis and numerical simulation. The impact of finite molecular volume is dominant but the intermolecular attraction force further stabilizes the detonation. Accordingly, the regularity of the cellular structure was greatly enhanced, and fully planar detonation could be observed in the simulation with RK gas.

4 Acknowledgements

Zhuyin Ren acknowledges the financial support from National Natural Science Foundation of China (52025062).

References

[1] Bourlioux, A. (1991). Numerical study of unstable detonations. Ph.D. thesis, Princeton University.

[2] Erpenbeck, JJ. (1962). Stability of idealized one-reaction detonations. Phys. Fluids, 5(5):604.

[3] Erpenbeck, JJ. (1964). Stability of steady-state equilibrium detonations. Phys. Fluids, 7(5):684.

[4] Gorchkov V, Kiyanda C, Short M, Quirk J. (2007). A detonation stability formulation for arbitrary equations of state and multi-step reaction mechanisms. Proc. Combust. Inst., 31(2):2397–2405.

[5] Lee HI, Stewart DS. (1990). Calculation of linear detonation instability: one-dimensional instability of plane detonation. J. Fluid Mech., 216:103–132.

[6] Pintgen F, Eckett C, Austin J, Shepherd J. (2003). Direct observations of reaction zone structure in propagating detonations. Combust. Flame, 133(3):211–229.

[7] Sharpe F, Sharpe SAEG. (2000). Two-dimensional numerical simulations of idealized detonations. Proc. R. Soc. Lond. A, 456(2001):2081–2100.

[8] Sharpe GJ, Quirk JJ. (2008). Nonlinear cellular dynamics of the idealized detonation model: Regular cells. Combust. Theory Modell., 12(1):1–21.

[9] Short M, Stewart DS. (1998). Cellular detonation stability. Part 1. A normal-mode linear analysis. J. Fluid Mech., 368:229–262.

[10] Taileb S, Melguizo-Gavilanes J, Chinnayya A. (2021). The influence of the equation of state on the cellular structure of gaseous detonations. Phys. Fluids, 33:036105.

[11] Weng Z, Mével R. (2023). Implementation of an OpenFOAM solver for shock and detonation simulation at high pressure. Comput. Fluids, 265:106012.

[12] Weng Z, Mével R. (2024). Dynamics of detonation cellular structure in linear and nonlinear instability regimes. Proc. Combust. Inst., 40(1):105438.

[13] Weng Z, Mével R. (2024). Linear and non-linear stability of gaseous detonation at elevated pressure. Combust. Flame, 262:113361.